Journal of Hydroinformatics

Journal of Hydroinformatics Vol 25 No 4, 1312 doi: 10.2166/hydro.2023.202

Rotary gate discharge determination for inclusive data from free to submerged flow conditions using ENN, ENN–GA, and SVM–SA

Ava Marashi[a], Salah Kouchakzadeh [b,*] and Hojjat Allah Yonesi[c]

[a] Ph.D. Graduate, Department of Water Engineering, College of Agriculture, Lorestan University, Iran
[b] Irrigation and Reclamation Eng. Dept., University of Tehran, P.O. Box 31587-4111, Karaj 31587-77871, Iran
[c] Department of Water Engineering, College of Agriculture, Lorestan University, Lorestan, Iran
*Corresponding author. E-mail: skzadeh@ut.ac.ir

SK, 0000-0002-3752-943X

ABSTRACT

This study aims at evaluating the performance of the Elman Neural Network (ENN), Elman Neural Network-Genetic Algorithm (ENN–GA), and Support Vector Machine-simulated annealing (SVM–SA) in determining the discharge of a newly proposed rotary gate for the inclusive data range from free flow to highly submerged conditions. For individual free and submerged flows, the models performed as well as that of the traditional relationships. However, the superiority of the intelligent models comes when dealing with the inclusive data set of both flow conditions, where no deterministic approach is available for discharge evaluation prior to specifying the threshold condition. In such complex flow conditions, the ENN–GA hybrid model with a proper structure determined the discharge with rather a high accuracy, i.e., SE of 6.12%. Also, in defining the threshold state, the ENN and ENN–GA models achieved superior results compared to the currently available relationship, i.e., it accurately recognized the threshold condition in almost 100% of the cases while the traditional relationship results were limited to 93% of the cases. Such accuracy of the employed model in assessing the discharge of the structure and its high ability in recognizing the flow state could be of great advantage for irrigation network structure automation.

Key words: ENN, ENN–GA, flow condition, rotary gate, semicircular canal, SVM–SA

HIGHLIGHTS

- Application of the ENN, ENN-GA, SVM-SA to determine the flow parameters of the new rotary gate in free, submerged flow conditions, and more importantly the inclusive data from free to highly submerged state which was examined for the first time in this research.
- To recognize the complex threshold flow between free and submerged conditions and the proposed Artificial Intelligence models with more than 98% accuracy which is crucial in field conditions and for gate automation.

GRAPHICAL ABSTRACT

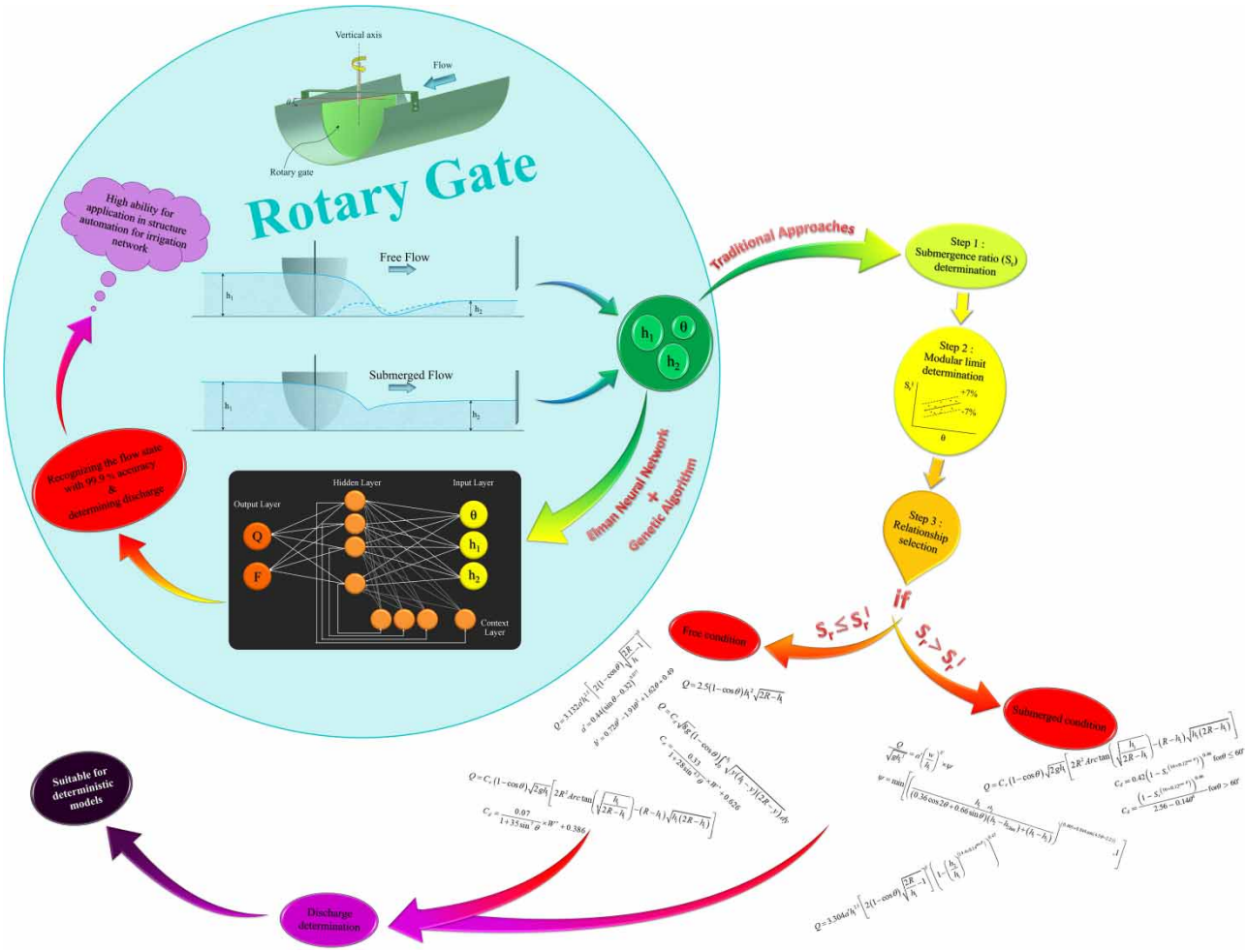

1. INTRODUCTION

Gates of various types have been used for water surface regulation and flow measurement and delivery in irrigation networks. The hydraulic performance of such gates has been studied in free and submerged flow conditions for providing discharge coefficients and stage–discharge relationships. Application of conventional sluice and tainter gates in elevated precast concrete canals with semicircular and semielliptical cross-sections imposes additional construction costs for structure installation and increases maintenance expenses. Accordingly, Marashi *et al.* (2021a, 2021b) proposed the rotary gate for semicircular cross-section canals and reported its hydraulic performance. The main advantage of the rotary gate over the conventional sluice gate is the movement around its vertical axis of symmetry, which assists its maneuver and decreases the required force for rotation because of the rather balanced pressure at the sides of the symmetry axis. This could be considered a great advantage for network automation. Also, it could be considered a self-cleaning gate because both the floating debris and the carried sediment could easily be transported to the downstream side of the gate.

This novel structure was designed as a regulating device, i.e., it is used for regulating the upstream water stage for offtake purposes and for evaluating the inline passing flow rate. Discharge determination in such a structure is related to the upstream and downstream flow depth, which could easily and accurately be measured. That is, the discharge is indirectly evaluated by using the flow depths and associated hydraulic relationships. The passing flow could be in a free state or a submerged one, accordingly, different relationships govern each flow state. consequently, the accuracy of the discharge evaluation highly depends on the precise determination of the threshold condition of the flow submergence, which in turn assists in the selection of the proper formula.

The hydraulic performance of the gate in free and submerged flow conditions was theoretically and experimentally studied to develop relationships for determining the flow rate and discharge coefficient in both flow conditions (Marashi *et al.* 2021a, 2021b). Three approaches were used in the study, i.e., using basic principles, applying dimensional analysis, and using the superposition principle. Good agreements between the proposed relationships and the compiled data were got and reported independently for both free and submerged flow conditions.

The aim of the present study is to apply a data science means to recognize the flow states, i.e., free, threshold, and submerged conditions, and to determine the flow rate accordingly with the desired accuracy. Such a method could be used in the process of gate automation with great success. Data science and machine learning (ML) tools have been successfully used for determining the flow rate of various structures, including the use of three ML models, i.e., Gaussian Process Regression (GPR), Generalized Regression Neural Network (GRNN), and Multi-Gene Genetic Programming (MGGP) to predict the discharge coefficient of radial gates in free and submerged conditions individually (Tao *et al.* 2022). Also, the Artificial Neural Networks (ANNs), support vector machine (SVM), Random Forest (RF), Random Tree (RT), GPR, and GRNN were applied to determine the flow rate and discharge coefficient of vertical and oblique sluice gates in free and submerged conditions (Rady 2016; Salmasi *et al.* 2021).

The performance of several artificial intelligence (AI) methods, including Deep Learning (DL), RF, General Linear Model (GLM), and Boost Gradient Machine (BGM), for determining the sluice gate discharge coefficient were investigated (Ghorbani *et al.* 2020). Also, AWARD (Appropriate Weir Adjustment with Water Requirement Deliberation) model, which integrates neural network and ML techniques for water level prediction, and sluice gates settings, was developed by Suntaranont *et al.* (2020). Furthermore, Nouri & Hemmati (2020) employed Recurrent Neural Networks (RNNs), Convolutional Neural Networks (CNNs), and Multi-Layer Perceptron (MLP) networks to determine the discharge coefficient of the weir gate structures. Ayaz & Mansoor (2018) evaluated the discharge coefficients of oblique sharp-crested weirs for free and submerged flow conditions using an ANN model.

Zhang & Yuan (2008) suggested the genetic algorithm (GA) to adjust the Elman neural network's (ENN) starting weights, leading to the creation of a powerful GA-Elman dynamic recurrent neural network stock prediction model which could be used for stock price prediction. Xing *et al.* (2022), to improve the water level prediction performance, developed a new hybrid model strategy based on the VMD double processing, ENN–GA, and ARIMA prediction. The results showed that the coupled model provided a better prediction performance than that of the traditional one. Yao *et al.* (2018) used the GA to optimize the weights of the ENN to predict the water level of the Yongding River monitoring site. They obtained higher efficiency by using the ENN–GA compared to that of the ENN. Ding *et al.* (2013) used GAs to improve the weights, thresholds, and number of hidden layer neurons of Elman networks, which increased the ENNs' training speed and accuracy.

Many studies have shown the potential of SVM models, and their effective and reliable performance in different investigations which made them desirable AI choices for applications (Yaghoubzadeh-Bavandpour *et al.* 2022). Such a model outlines the separation between classes and maps of the input space formed by independent variables with nonlinear transformation under the kernel function (Przybył & Koszela 2023). Several studies have suggested various hybrid SVM designs to improve SVM efficiency. Samantaray *et al.* (2023) investigated the effectiveness of SVM, backpropagation neural network (BPNN), and integration of SVM with particle swarm optimization (PSO–SVM) models for flood forecasting. It was found that PSO–SVM could be used as a better choice for flood forecasting, as it offered a higher level of dependability and precision. Zaini *et al.* (2018) employed a hybridized SVM–PSO model for forecasting daily river flow at the Upper Bertam watershed. Their results showed that the SVM–PSO model was superior to the basic SVM model and provided more accurate results. Mehrabani Bashar *et al.* (2023) conducted a study on the influence of factors on rural drinking water demand, using the adaptive neuro-fuzzy inference system (ANFIS) and hybrid models, such as ANFIS–GA, ANFIS–PSO, and SVM–SA. Analysis of the results of the various models showed that SVM–SA was the most successful.

The literature indicates that previous research works concerning control and measurement structures focused only on studying free and submerged flow conditions separately. While the ability of the employed AI method to determine the flow condition, i.e., recognizing the free flow condition from the complex submerged one, is crucial in such studies. Especially, the case is getting more important in the case of the rotary gate with a rather complex flow field where two released right and left jets collide at the downstream side of the gate, which generates a unique flow condition among other control structures. Such a unique flow condition of the rotary gate makes the determination of the distinguishing curve between the free and submerged flow conditions entirely different from that of other structures, which calls for in-

depth investigation. In this study, the ability of the AI models to identify the flow condition and to determine the flow parameters of the rotary gate was tested, and the results were compared with the output of the gate's traditional relationship.

2. EXPERIMENTAL SETUP

The data were compiled in a 0.664 m diameter semicircular flume 12 m long constructed of rolled galvanized iron sheets installed on a steel frame. The experimental setup was built in the Central Hydraulic Laboratory, Irrigation and Reclamation Engineering Department at the University of Tehran.

The semicircular rotary gate was made of a 4 mm thick iron sheet and sharp-edged by a CNC machine. The gate was attached to a metal frame and placed in the flume (Marashi *et al.* 2021a). The opening angle of the gate was adjusted by the user with the rotation around the vertical axis of symmetry and was fixed in place by two screws. The opening angles could be adjusted between 0° and 90°, which, respectively, indicate a fully closed and fully opened gate. The submerged flow was also established by adjusting a sluice gate opening installed at the downstream end of the semicircular flume.

The flume was supplied with water via a 150 mm diameter pipe from a large elevated constant head tank, and the flow rate was measured by an electromagnetic flowmeter with 0.5% accuracy mounted on the feeding pipe. The feeding pipe ended with a perforated pipe installed at the flume entrance to reduce the flow turbulence.

The flow depth in the flume was measured by using 16 pressure transmitters with 0.5% accuracy. Also, a piezometer board was used for calibrating the transmitters *in situ*. Figure 1 shows a plan view of the experimental setup, and Figure 2 shows a 3D schematic of the installed rotary gate. The flow characteristics were recorded for a discharge range between 0.002 and 0.07 m^3s^{-1} and for gate opening angles from 20° to 80°. The free and submerged conditions were labeled 0 and 1, respectively. Table 1 presents the range of studied parameters.

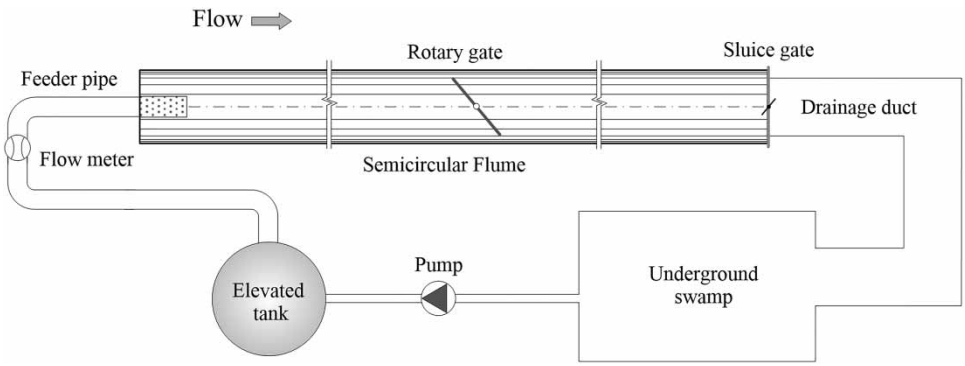

Figure 1 | Schematic plan of the experimental setup.

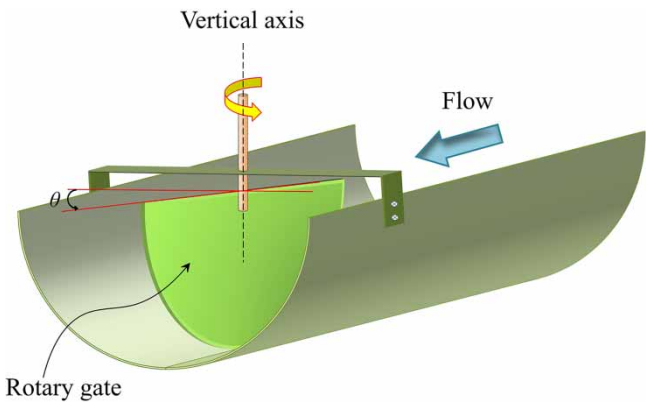

Figure 2 | Three-dimensional schematic view of the rotary gate.

Table 1 | The range of the studied parameter

Parameter	Units	Range
Discharge	m^3s^{-1}	0.002–0.07
Gate opening angle	Radians	0.349–1.396
Upstream flow depth	m	0.041–0.319
Tailwater depth	m	0.035–0.308
Flow condition label	–	0 for free condition 1 for submerged condition

3. FLOW MOVEMENT AROUND THE GATE IN FREE AND SUBMERGED CONDITIONS

Because of the gate design, two jets of the flowing water left the openings of the gate and collided at the downstream side, as presented in Figure 3(a). Experimental observations showed that a relatively large hump was generated due to the jets' collision and an oblique-like hydraulic jump occurred in the hump's vicinity position. This phenomenon caused considerable energy dissipation downstream of the rotary gate.

The flow rate in a free flow condition is only affected by the opening angle and the upstream flow depth, i.e., in such flow condition, the downstream depth does not influence the flow rate. Increasing the tailwater depth, however, drowns the collision hump and leads to gate submergence (Figure 3(b)), which affects the upstream flow depth and the released discharge.

In the submerged condition, a higher upstream flow depth than that of the free flow is required to release a given discharge. In other words, gate submergence reduces the flow rate for a specific upstream flow depth. The intensity of the submergence is usually expressed by the submergence ratio, defined as the ratio of the tailwater depth to the upstream depth of the gate. For a gate opening angle and a specific upstream flow depth, increasing the submergence ratio decreases the discharge, and as the submergence ratio approaches unity, the discharge tends to zero. This reveals that the flow rate could not be determined by using only the upstream depth. Indeed, different formulations and approaches are used for evaluating the discharge in free and submerged flow conditions. Therefore, correctly identifying the flow type for accurate flow measurements and water delivery is a key point for such a structure, especially when it comes to irrigation network automation. In such complicated conditions, the application of intelligent systems could be of great assistance, especially because they could override the difficulty of shifting from one formulation to another when the flow condition is changed. Also, they could increase the accuracy of flow computation in the marginal threshold band between these flow conditions. Furthermore, such a means could be incorporated into an automated gate control system.

4. GOVERNING EQUATIONS

4.1. Discharge determination approaches in free flow condition

In free flow conditions, the discharge of the rotary gate is related to the upstream depth and the opening angle. Two methods, i.e., applying the dimensional analysis and using the basic principles, were considered developing the discharge equations in

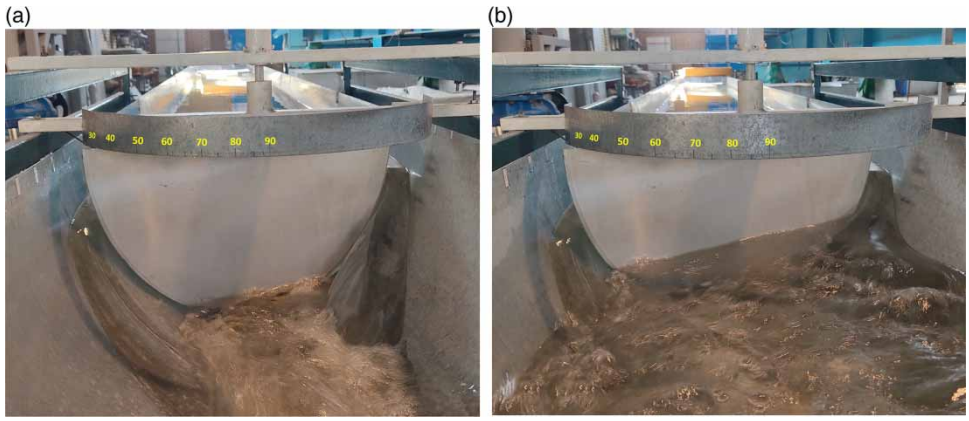

Figure 3 | Flow in downstream of the rotary gate: (a) free flow condition and (b) submerged flow condition.

free flow condition. In the dimensional analysis approach, based on two dimensionless parameters, i.e., $Q^* = [Q/(gh_1^5)^{0.5}]$ and $W^* = w/h_1$, Equations (1) and (2) were obtained; the latter, however, provided marginally higher accuracy (Marashi *et al.* 2021a).

$$Q = 2.5(1 - \cos\theta)h_1^2\sqrt{2R - h_1} \tag{1}$$

$$Q = 3.132a'h_1^{2.5}\left[2(1 - \cos\theta)\sqrt{\frac{2R}{h_1} - 1}\right]^{b'} \tag{2}$$

where Q, g, h_1, w, θ, and R are discharge, gravitational acceleration, upstream flow depth, cross-section flow width at the water surface, opening angle and gate radius, respectively, and Equations (3) and (4) provide a' and b' values.

$$a' = 0.44(\sin\theta - 0.32)^{0.077} \tag{3}$$

$$b' = 0.72\theta^3 - 1.91\theta^2 + 1.62\theta + 0.49 \tag{4}$$

In the second approach, the basic principles were applied and based on the overflow and underflow structures concept, Equations (5) and (7) were obtained, respectively.

$$Q = C_d\sqrt{8g}(1 - \cos\theta)\int_0^{h_1}\sqrt{y(h_1 - y)(2R - y)}.dy \tag{5}$$

where y is the vertical distance from bottom and C_d is the discharge coefficient which could be determined by using Equation (6)

$$C_d = \frac{0.33}{1 + 28\sin^{4.3}\theta} \times W^* + 0.626 \tag{6}$$

$$Q = C_d(1 - \cos\theta)\sqrt{2gh_1}\left[2R^2 Arc\tan\left(\sqrt{\frac{h_1}{2R - h_1}}\right) - (R - h_1)\sqrt{h_1(2R - h_1)}\right] \tag{7}$$

where C_d could be determined by using Equation (8)

$$C_d = \frac{0.07}{1 + 35\sin^7\theta} \times W^* + 0.386 \tag{8}$$

Comparison between observed and calculated values indicated both equations provided the same order of accuracies. However, the solution of Equation (5) requires numerical integration, while Equation (7) could easily be used.

4.2. Discharge determination approaches in submerged flow conditions

In submerged flow, the tailwater depth affects the flow rate. Therefore, the discharge is related to the gate opening angle, the upstream depth of the gate, and the tailwater depth. Two approaches were used by Marashi *et al.* (2021b) to evaluate the

submerged discharge, i.e., the superposition and the dimensional analysis, which yielded Equations (9) and (10), respectively.

$$Q = 3.304a'h_1^{2.5}\left[2(1-\cos\theta)\sqrt{\frac{2R}{h_1}-1}\right]^{b'}\left(1-\left(\frac{h_2}{h_1}\right)^{(14.4\times 0.14^{\cos\theta})}\right)^{0.47} \tag{9}$$

$$\frac{Q}{\sqrt{gh_1^5}} = a'\left(\frac{w}{h_1}\right)^{b'}\times\psi$$
$$\psi = \min\left[\left(\frac{h_1-h_2}{(0.36\cos 2\theta + 0.66\sin\theta)(h_2-h_{2\,\mathrm{lim}})+(h_1-h_2)}\right)^{(0.405+0.044\cos(4.5\theta-2.2))}, 1\right] \tag{10}$$

where a' and b' could be determined by using Equations (3) and (4) (Marashi *et al.* 2021b).

They also proposed a linear relationship (Equation (11)) for the modular limit or the submergence threshold condition for the rotary gate.

$$\frac{h_{2\,\mathrm{lim}}}{h_{1\,\mathrm{lim}}} = 0.45\theta + 0.194 \tag{11}$$

where h_2 is the tailwater depth, $h_{2\mathrm{lim}}$ is the tailwater depth at the submergence threshold condition and $h_{1\mathrm{lim}}$ is the upstream flow depth of the gate in the free flow condition, which could be determined by using Equation (2).

The submergence threshold condition should be determined to classify the flow state based on which the proper formulation for discharge computation should be applied. If the submergence ratio for a flow condition is less than or equal to the threshold value, the free flow condition prevails; otherwise, the submerged condition exists.

5. RESEARCH METHODOLOGY

5.1. Elman neural network: utilized function and structure

In this study, a multilayer neural network, termed ENN, proposed by Elman (1990), was used to specify the flow condition and to determine the flow rate through a rotary gate installed in a semicircular canal. This neural network has been successfully applied in many fields associated with prediction, modeling, and control (Sheela & Deepa 2013). The ENN is a dynamic recurrent neural network and consists of an input layer, a hidden layer, an output layer, and a context layer. The context layer is a feedback connection from the hidden layer to the input layer; it records information from the last network iteration and feeds it as input to the current iteration (Li *et al.* 2019). Jia *et al.* (2014) attributed the advantage of the ENN over other ANN models to the ability of memorization and the characteristic of being time-varying features, which leads to stronger global stability. Also, Kumar *et al.* (2021) believed that ENN is more efficient than other ANN models due to its capability of learning different complex pattern in a specific data set. Accordingly, the ENN model was chosen for the study of the complex data set of the flow conditions from free to highly submerged one.

In the present study, the hidden layer transfer function, the adaptation learning function, and the network training function were selected as TANSIG, LEARNGDM, and TRAINLM, respectively.

The neural network structure was selected based on that proposed by Ke & Liu (2008). They proposed Equation (12) for determining the optimum number of neurons.

$$N_n = \frac{N_{in}+\sqrt{N_p}}{L} \tag{12}$$

where N_n is the number of neurons, L is the number of the hidden layers, N_{in} is the number of inputs, N_p is the number of input samples.

5.2. Hybrid models

Hybrid simulation has become vastly more popular over the past two decades (Brailsford *et al.* 2019). A hybrid simulation–optimization model is a modeling approach that combines simulation and optimization techniques to solve complex

problems. Hybrid simulation–optimization methods have enabled an exploration of the complexities of planning and scheduling issues. In this study, the accuracy of the following hybrid models was evaluated in determining discharge and recognizing the flow condition:

5.2.1. ENN–GA

The ENN usually applies the gradient descent arithmetic for training and learning, causing the error function to be continuously differentiable so that resolving the problem can move from the current position in the search space to another position toward the inverse of the error gradient, and the search direction is relatively low. The selection of the initial weights and values heavily influences the performance of the network. However, the initial values are chosen randomly. An inappropriate selection in complex or multi-maximum data can lead the neural network to settle in the local optimum state. Recently, a GA was used to optimize the initial weights and biases and to enhance the performance of the ENN prediction. This hybrid algorithm has shown superior effectiveness and computational performance over traditional methods (Ding *et al.* 2013).

5.2.2. SVM–SA

An intelligent model, SVM is a powerful classification tool that has been growing in popularity. This method is popular for small-sample, nonlinear, and high-dimensional pattern recognition problems (Zhou *et al.* 2021). To enhance SVM's performance, γ and σ would have initial values based on the input. The Simulated Annealing (SA) algorithm was then employed to calculate the best values of these parameters. Based on a fitness function, these values had converged to an optimal value. The model output was calculated when the values were put into the SVM model (Mehrabani Bashar *et al.* 2023).

5.3. Data normalization technique

To improve the neural network performance and increase its output accuracy, all the required data, which include gate opening angle, upstream and tailwater flow depth, and the discharge, were normalized using Equation (13) (Salas *et al.* 1980):

$$x_{nor} = a(x - b)^c \tag{13}$$

where x_{nor} is the normalized data, x is the original data, and the constants a, b, and c were determined by setting the series skewness of each parameter equal to zero.

5.4. Models' performance evaluation method

To evaluate the performance of the models and determine the errors associated with its calculated discharge, Q_c, regarding the observed values, Q_o, the widely used statistical parameters including the Average Relative Error (ARE), the Root Mean Square Error (RMSE), the Standard Error (SE), and the Normal Root Mean Square Error (NRMSE) were used which, respectively, defined by Equations (14)–(17).

$$\text{ARE} = \frac{\sum \left| \frac{Q_o - Q_c}{Q_o} \right|}{N_p} \times 100 \tag{14}$$

$$\text{RMSE} = \sqrt{\frac{\sum (Q_o - Q_c)^2}{N_p - 1}} \tag{15}$$

$$\text{SE} = \frac{\text{RMSE}}{\bar{Q}_o} \times 100 \tag{16}$$

$$\text{NRMSE} = \frac{\text{RMSE}}{Q_{o\_\max} - Q_{o\_\min}} \times 100 \tag{17}$$

where Q_{o_max} is the maximum observed discharge, and Q_{o_min} is the minimum observed discharge, other parameters were previously defined. The mentioned indicators were chosen to compare the results of the current study with that of previous research in which they were employed.

5.5. Accuracy of the results

To evaluate the accuracy of the results, two statistical parameters, including the Average Relative Interval Length (ARIL) and the Percentage of the Observation Coverage (POC) defined by Equations (18) and (19) were used (Jin *et al.* 2010; Ahmadi *et al.* 2019):

$$\mathrm{ARIL} = \frac{1}{N_p}\sum \frac{Q_{c-\max} - Q_{c-\min}}{Q_o} \tag{18}$$

$$\mathrm{POC} = \frac{\mathrm{NQ_{in}}}{\mathrm{NQ_o}} \times 100 \tag{19}$$

where $Q_{c\text{-max}}$ and $Q_{c\text{-min}}$ are the calculated upper and lower confidence limits of the chosen discharge, respectively, $\mathrm{NQ_{in}}$ is the number of observed discharges falling in the confidence interval, and $\mathrm{NQ_o}$ is the number of observed discharge values. Closest ARIL values to zero and simultaneously higher POC values up to 100% indicate a better performance of the model.

5.6. Study processing

In this research, three stages were followed to reach the best structure in the ENN. In each stage, 80% of the data was used for training the network and 20% for evaluating the results. In the first stage, the free flow condition was investigated in which the upstream flow depth and the gate opening angle were the inputs, and the discharge was the output of the model. The submerged flow was investigated in the second stage, in which the inputs were the flow depth at the upstream side of the rotary gate, the tailwater depth, and the gate opening angle, and the output was the submerged discharge. In the third stage, the complete set of data, i.e., free and submerged flow conditions, was used in the analysis. In this stage, the inputs included the upstream flow depth, the tailwater depth, and the gate opening angle, and the outputs were the discharge and the flow condition label. In the third stage, the main purpose of training the models was to recognize the flow condition and to properly determine the discharge accordingly. To the writer's knowledge, such analysis, i.e., identifying the flow condition of a control structure, was not published yet. Such ability of an intelligent model in case of success could be of great advantage in irrigation network automation.

6. DISCUSSION AND RESULTS

6.1. The models' performance in free flow conditions

Both of ENN and ENN–GA were trained for free flow condition with five neurons in two hidden layers. The number of layers and neurons was selected according to Equation (12) using 60 input data points. The models training and testing were repeated 20 times for random arrangements of 80 and 20% of the data for the training and verification stages of the models. Figure 4 shows a sample output of all models training and verification results for discharge calculation. The statistical parameters associated with the results are computed and tabulated in Table 2 and compared with the results of hydraulic approaches. The table shows that using hybrid models for free condition performed as good as that of the traditional relationships.

6.2. Models' performance in submerged flow conditions

ENN and ENN–GA training for submerged flow condition was performed with two structures of seven neurons in two hidden layers and five neurons in three hidden layers. The number of layers and neurons of both structures was selected according to the input data using Equation (12). The models training and evaluation were repeated 20 times for 80 and 20% of the data, respectively, that were arranged randomly. Figure 5 shows the output of all models training and verification results for discharge calculation in submerged flow condition. Table 3 represents the averages of statistical parameters associated with the results of the models and the results of the previously proposed equation for calculating the submerged discharge. The table shows that the applied models for the submerged condition performed almost as good as that of the traditional relationships.

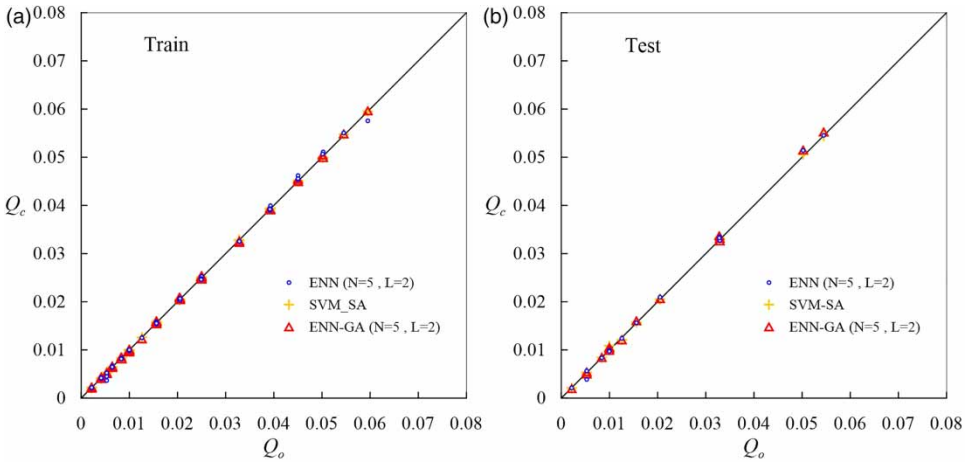

Figure 4 | Model's performance for free discharge evaluation during: (a) training stage and (b) evaluation stage.

Table 2 | Statistical parameters indicating the performance of different approaches for free discharge evaluation

Approach		ARE (%)	RMSE (m^3s^{-1})	SE (%)	NRMSE (%)
Single trend line [Equation (1)]		3.45	0.0012	6.29	2.08
Individual opening angle [Equation (2)]		1.38	0.0003	1.87	0.62
Overflow [Equation (5)]		1.02	0.0002	1.11	0.37
Underflow [Equation (7)]		1.29	0.0002	1.22	0.4
ENN	Train	1.79	0.0005	2.5	0.86
Structure: N = 5, L = 2	Test	2.59	0.0006	3.03	1.23
SVM–SA	Train	0.4	0.0001	0.47	0.15
	Test	1.46	0.0003	1.67	0.65
ENN–GA	Train	1.45	0.0002	1.20	0.39
Structure: N = 5, L = 2	Test	2.62	0.0006	2.81	1.09

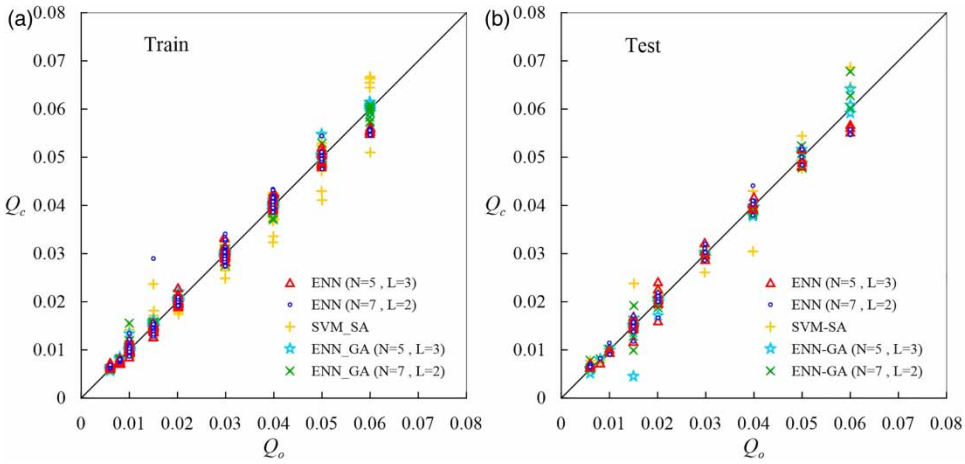

Figure 5 | Performance of the ENN and the hybrid models for submerged discharge evaluation: (a) training stage and (b) evaluation stage.

6.3. Models' performance based on inclusive data set

In the third stage of the study, the complete set of data, covering the whole range from free flow to highly submerged conditions, was used for evaluating performance of the models in the more complex and practical situation. In this stage, the

Table 3 | Statistical parameters indicating the performance of different approaches for submerged discharge evaluation

Approach		ARE (%)	RMSE (m^3s^{-1})	SE (%)	NRMSE (%)
Superposition [Equation (9)]		2.35	0.0007	3.87	1.67
Pi theorem [Equation (10)]		1.54	0.0005	2.79	1.21
ENN	Train	4.28	0.0015	6.43	2.83
Structure: N = 5, L = 3	Test	6.31	0.0019	7.25	3.59
ENN	Train	5.12	0.0018	7.62	3.36
Structure: N = 7, L = 2	Test	6.93	0.002	7.56	3.75
SVM–SA	Train	5.01	0.0024	9.89	4.36
	Test	7.23	0.0031	11.6	5.75
ENN–GA	Train	1.93	0.0007	2.92	1.29
Structure: N = 5, L = 3	Test	4.99	0.0021	7.85	3.89
ENN–GA	Train	2.63	0.0009	3.82	1.68
Structure: N = 7, L = 2	Test	5.37	0.0020	7.58	3.75

gate opening angle and the upstream and tailwater depths of the rotary gate were the inputs, and the outputs were the discharge and the flow condition label. The ENN and ENN–GA were trained with two structures of nine neurons in two hidden layers and seven neurons in three hidden layers. The number of layers and neurons of both structures has been selected according to the number of input data values, using Equation (12). Eighty percent of the data points were used for training the models and the rest for evaluating its performance. Figure 6 shows the output of the models training and verification results for determining the rotary gate discharge. Table 4 presents the averages of statistical parameters associated with the results of the models for the whole data set. The table reveals that all models have almost a good performance in determining the discharge, although the ENN–GA hybrid model with seven neurons and three hidden layers presented the best performance compared to other models.

The violin graphs were plotted to evaluate the ENN, ENN–GA and SVM–SA models' performance in discharge determination. Figure 7 shows the violin plots for observed and computed values of discharge.

The plot indicates that the discharge evaluated using the ENN and ENN–GA with seven neurons in three hidden layers concurs with the observed values more than that obtained by other models.

Comparison of the models with observed values was also made based on Taylor diagrams in Figure 8. The Taylor diagrams evaluate the model's performance based on their standard deviations among observed and calculated values, correlation coefficient and RMSE values. Ideal values for the correlation coefficient and RMSE are 1 and 0, respectively. Obviously, the

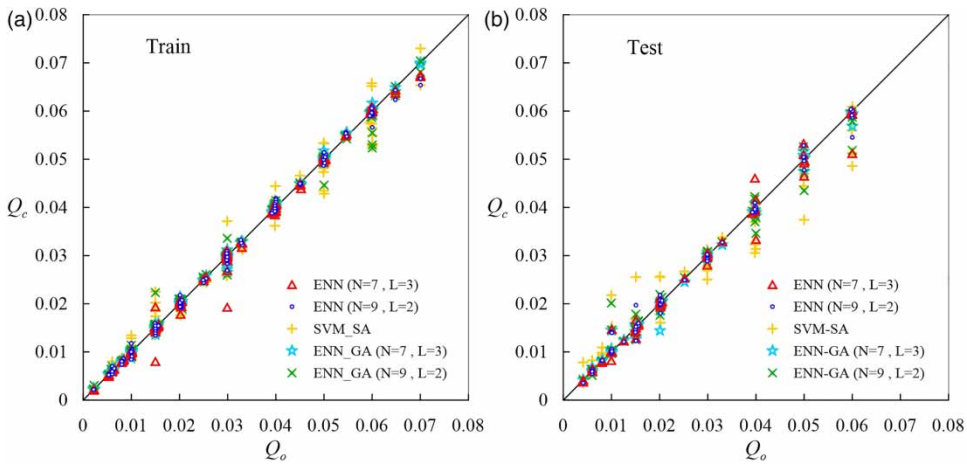

Figure 6 | Performance of ENN, ENN–GA, and SVM–SA models for the inclusive data range from free to submerged discharge: (a) training stage and (b) evaluation stage.

Table 4 | Statistical parameters indicating the performance of different models for discharge evaluation based on the whole data set from free flow to submerged conditions

Approach		ARE (%)	RMSE (m^3s^{-1})	SE (%)	NRMSE (%)
ENN	Train	3.24	0.001	4.27	1.56
Structure: N = 7, L = 3	Test	5.5	0.0016	6.34	2.85
ENN	Train	3.12	0.0011	4.51	1.65
Structure: N = 9, L = 2	Test	5.69	0.0016	6.44	2.9
SVM–SA	Train	4.36	0.0019	7.49	2.74
	Test	14.46	0.0043	17.02	7.66
ENN–GA	Train	2.01	0.0007	2.86	1.05
Structure: N = 7, L = 3	Test	4.87	0.0015	6.12	2.75
ENN–GA	Train	3.28	0.0013	5.23	1.92
Structure: N = 9, L = 2	Test	6.94	0.0023	9.22	4.15

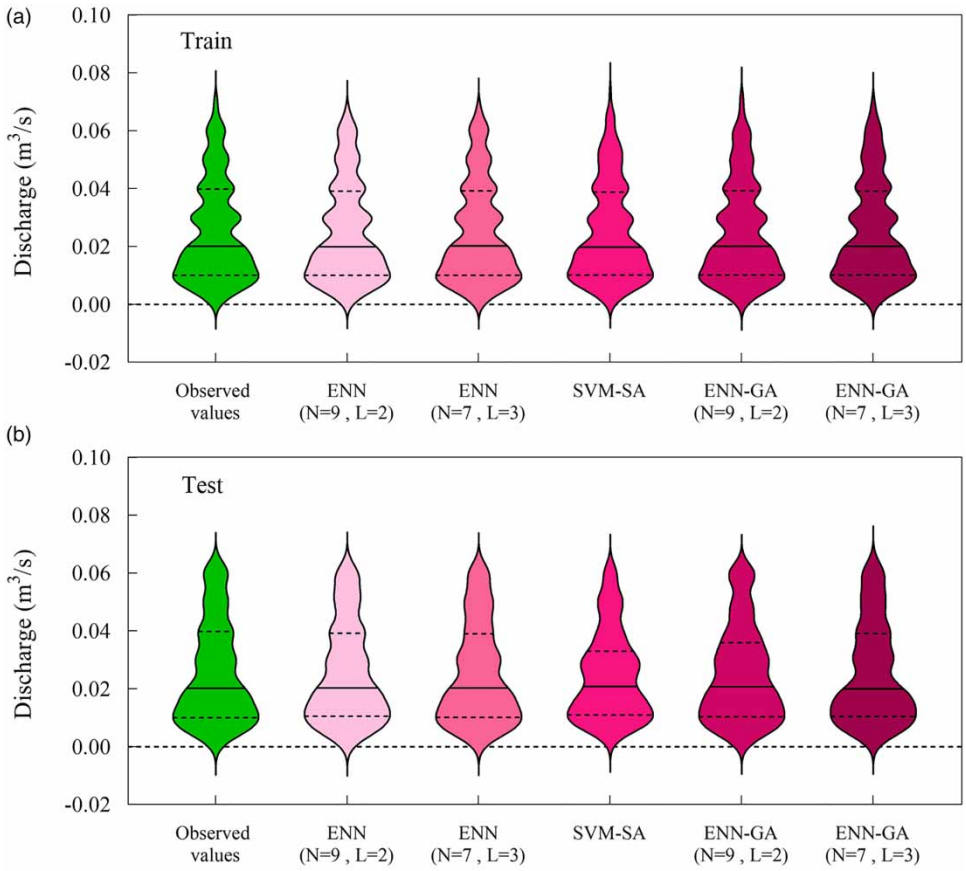

Figure 7 | Violin plots of ENN, ENN–GA, and SVM–SA models for the inclusive data range from free to submerged discharge: (a) training stage and (b) evaluation stage.

correlation coefficient of the observed values when compared with themselves would be unity. Therefore, its indicator, i.e., the black circle, would fall on the horizontal axis with correlation coefficient equals one and their inherent standard deviation. A model with the closer distance to such a point indicates the highest performance among other models. Figure 8(b) reveals that all models except SVM–SA generated outputs very close to the horizontal axis, i.e., high correlation

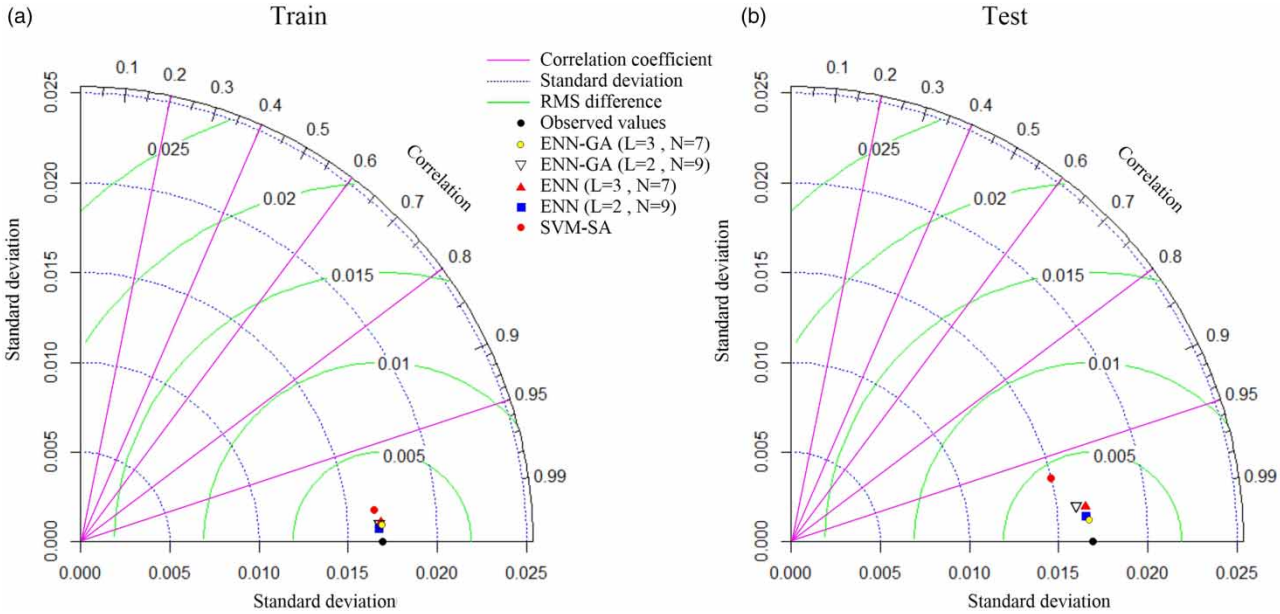

Figure 8 | Taylor diagram for ENN, ENN–GA, and SVM–SA models for the inclusive data range from free to submerged discharge: (a) training stage and (b) evaluation stage.

coefficient, with standard deviations in the range of the observed values. Although the ENN–GA hybrid model with seven neurons and three hidden layers performed marginally better, this diagram indicates the ENN and ENN–GA models could properly be employed for discharge determination in such complex flow conditions.

6.4. Evaluation of ENN and ENN–GA uncertainty in discharge determination

The Uncertainty bounds of the ENN and ENN–GA models for the two proposed structures are shown, respectively, in Figures 9 and 10.

The quality measure, ARIL, was used to evaluate the whole data set. Closer values of the ARIL to zero indicate a better performance of the model. In addition, the POC index, which represents the POC, was used to assess the accuracy of the model. A value of the POC close to 100% reveals that the model was able to cover more observational data. The results of ARIL and POC parameters were tabulated in Table 5.

A wide uncertainty band that includes all experimental data and its POC is close to 100 cannot indicate a good performance of the model, on the other hand, a narrow uncertainty band that is far from the observed data or includes few observed data is not a satisfactory situation, accordingly, the best model could be the one that yields a narrow uncertainty band and includes more observed data. A narrow uncertainty bound in Figure 10(b) with 0.107 and 83.6% for ARIL and POC, respectively, indicates the better performance of ENN–GA hybrid model with seven neurons and three hidden layers than others. As a result, the ENN–GA with a proper structure could determine the discharge accurately.

6.5. Elman neural network performance in identifying the flow conditions

As previously mentioned, precise identification of the flow condition is a vital step for accurate flow measurement in any flow measurement and control structures. Because changing the downstream flow condition could likely submerge the structure, in such a case the tailwater depth and its imposed submergence intensity drastically affect the flow rate. Therefore, only proper identification of the flow condition would ensue accurate flow measurement and sound management of control structures. This could be of higher importance where irrigation network component automation is considered. In this study, the ability of ENN, ENN–GA and SVM–SA models to recognize the flow condition was evaluated. The networks were used with two structures of seven neurons and three hidden layers, and nine neurons with two hidden layers. The flow condition was labeled 0 and 1 for free and submerged flow conditions, respectively. Eighty percent of the whole data set was used for training the network, and the rest of the data for evaluating its performance. The network training and evaluation were repeated 20 times. The results of the accuracy in recognizing the flow condition are tabulated in Table 6. The results showed that the

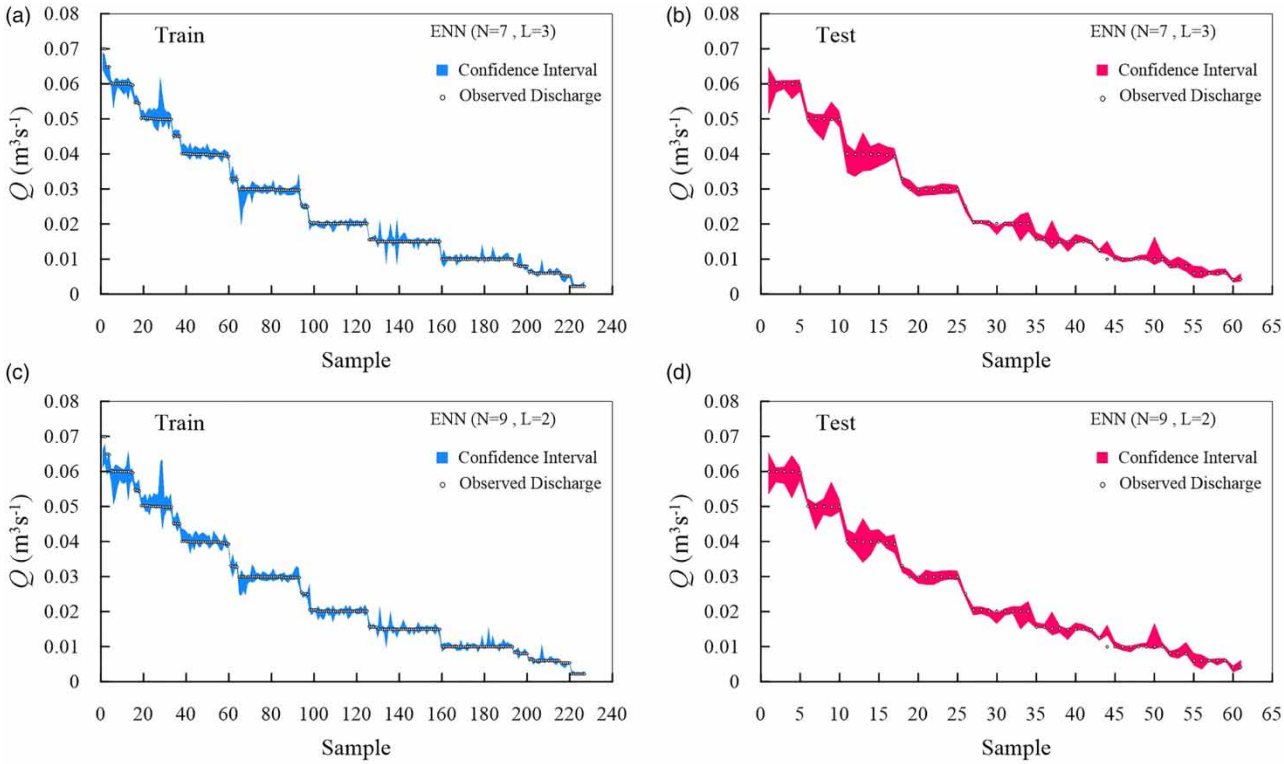

Figure 9 | Uncertainty bound of the employed ENN characteristics: (a) and (b) training and testing with seven neurons and three hidden layers, respectively; (c) and (d) training and testing with nine neurons and two hidden layers, respectively.

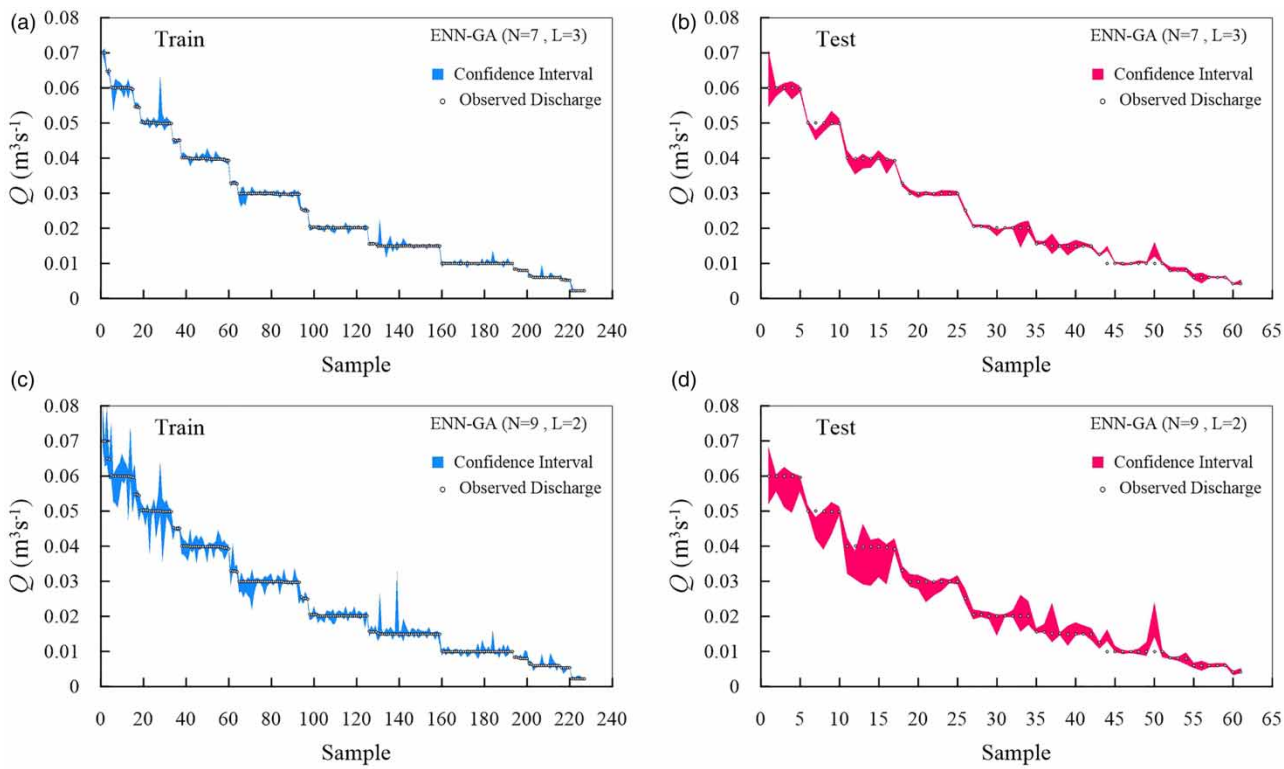

Figure 10 | Uncertainty bound of the employed ENN–GA characteristics: (a) and (b) Respectively training and testing with seven neurons and three hidden layers, (c) and (d) Respectively training and testing with nine neurons and two hidden layers.

Table 5 | Uncertainty indices in calculating discharge of the applied models characteristics

Approach		ARIL	POC (%)
ENN	Train	0.139	94.7
Structure: N = 7, L = 3	Test	0.188	93.4
ENN	Train	0.134	93.4
Structure: N = 9, L = 2	Test	0.193	88.5
ENN–GA	Train	0.076	88.5
Structure: N = 7, L = 3	Test	0.107	83.6
ENN–GA	Train	0.151	95.2
Structure: N = 9, L = 2	Test	0.218	91.8

Table 6 | Accuracy of the applied models in recognizing the flow conditions

Approach		Accuracy in recognizing the flow conditions (%)
ENN	Train	99.91
Structure: N = 7, L = 3	Test	99.92
ENN	Train	99.98
Structure: N = 9, L = 2	Test	99.84
SVM–SA	Train	100
	Test	98.36
ENN–GA	Train	100
Structure: N = 7, L = 3	Test	99.34
ENN–GA	Train	99.96
Structure: N = 9, L = 2	Test	99.84

difference in recognizing flow condition correctly is very marginal, i.e., the accuracy of SVM–SA model in recognizing the flow condition was 98.36% and that of the ENN and ENN–GA was higher than 99%. While the traditional relationships, i.e., Equation (11), accuracy for flow identification was limited to 93%. This reveals these intelligent models' performance was superior to the currently available relationships. Such performance would certainly be required for any automation program in the irrigation network.

7. CONCLUSION

Currently, different traditional relationships are used for determining discharge of regulating and flow measurement structures in free flow and submerged flow conditions. Selection of the proper relationship greatly depends on the accurate determination of the threshold flow condition. The main objective of this study was to examine the performance of the ENN, ENN–GA–GA and SVM–SA to determine the discharge of the rotary gate inclusively for the whole flow range from entirely free to highly intensive submerged condition. Also, they were employed to determine the threshold flow condition, i.e., the modular limit. The performance of the models was thoroughly evaluated in three stages for free flow, submerged flow, and the inclusive range of data from free to highly submerged condition. The results of the first two stages were compared with that of the traditional relationships, which showed that these models performed similar to that of the traditional relationships. While only the intelligence models are capable of dealing with the more complex whole data range from free to highly submerged flow. The performance of the models was highly accurate, especially when it comes to determining the threshold flow condition, they performed superior to that of the traditional relationships, i.e., the accuracy of the former was close to a 100% while the accuracy of the latter was limited to about 93% of the cases. Indeed, irrigation network structures automation demand high accuracy in determining flow conditions that would improve the water distribution across the network.

Due to the proper performance of the ENN and ENN–GA in evaluating the discharge and identifying the threshold flow condition accurately, they could be proposed for application in the control algorithm of the rotary gate for structure

automation. Obviously, the results are limited to the studied structure, i.e., the rotary gate. However, due to the sound performance of these models in evaluating the discharge for the entire flow range from free flow to highly submerged condition, it is recommended to study their application for other control and discharge measurement structure which would facilitate the application of structures automations.

ACKNOWLEDGEMENTS

The research was carried out in the Central Water Research Laboratory of the Irrigation and Reclamation Engineering Department, University of Tehran. The facilities provided by University of Tehran were highly appreciated.

DATA AVAILABILITY STATEMENT

All relevant data are provided in an Excel file as Supplementary Information.

CONFLICT OF INTEREST

The authors declare there is no conflict.

REFERENCES

Ahmadi, A., Nasseri, M. & Solomatine, D. P. 2019 Parametric uncertainty assessment of hydrological models: coupling UNEEC-P and a fuzzy general regression neural network. *Hydrological Sciences Journal* **64** (9), 1080–1094. https://doi.org/10.1080/02626667.2019.1610565.

Ayaz, M. & Mansoor, T. 2018 Discharge coefficient of oblique sharp crested weir for free and submerged flow using trained ANN model. *Water Science* **32** (2), 192–212. https://doi.org/10.1016/j.wsj.2018.10.002.

Brailsford, S. C., Eldabi, T., Kunc, M., Mustafee, N. & Osorio, A. F. 2019 Hybrid simulation modeling in operational research: a state-of-the-art review. *European Journal of Operational Research* **278** (3), 721–737. https://doi.org/10.1016/j.ejor.2018.10.025.

Ding, S., Zhang, Y., Chen, J. & Jia, W. 2013 Research on using genetic algorithms to optimize Elman neural networks. *Neural Computing and Applications* **23**, 293–297. https://doi.org/10.1007/s00521-012-0896-3.

Ghorbani, M. A., Salmasi, F., Saggi, M. K., Bhatia, A. S., Kahya, E. & Norouzi, R. 2020 Deep learning under H2O framework: a novel approach for quantitative analysis of discharge coefficient in sluice gates. *Journal of Hydroinformatics* **22** (6), 1603–1619. https://doi.org/10.2166/hydro.2020.003.

Jia, W., Zhao, D., Shen, T., Tang, Y. & Zhao, Y. 2014 Study on optimized Elman neural network classification algorithm based on PLS and CA. *Computational Intelligence and Neuroscience* 1–13. https://doi.org/10.1155/2014/724317.

Jin, X., Xu, C. Y., Zhang, Q. & Sing, V. P. 2010 Parameter and modeling uncertainty simulated by GLUE and a formal Bayesian method for a conceptual hydrological model. *Journal of Hydrology* **383** (3–4), 147–155. https://doi.org/10.1016/j.jhydrol.2009.12.028.

Ke, J. & Liu, X. 2008 Empirical analysis of optimal hidden neurons in neural network modeling for stock prediction. In: *IEEE Pacific-Asia Workshop on Computational Intelligence and Industrial Application 2*, pp. 828–832. https://doi.org/10.1109/PACIIA.2008.363.

Kumar, P., Lai, S. H., Mohd, N. S., Kamal, M. R., Ahmed, A. N., Sherif, M., Sefelnasr, A. & El-shafie, A. 2021 Enhancement of nitrogen prediction accuracy through a new hybrid model using ant colony optimization and an Elman neural network. *Engineering Applications of Computational Fluid Mechanics* **15** (1), 1843–1867. doi:10.1080/19942060.2021.1990134.

Li, C., Zhu, L., He, Z., Gao, H., Yang, Y., Yao, D. & Qu, X. 2019 Runoff prediction method based on adaptive Elman neural network. *Water* **11** (6), 1113. https://doi.org/10.3390/w11061113.

Marashi, A., Kouchakzadeh, S., Yonesi, H. A. & Torabi-Poudeh, H. 2021a Hydraulics of rotary gate: novel structure for semicircular canals. *Journal of Irrigation and Drainage Engineering* **147** (4), 04021003. https://doi.org/10.1061/(ASCE)IR.1943-4774.0001537.

Marashi, A., Kouchakzadeh, S., Rashidi, N. & Yonesi, H. A. 2021b Rotary gate: submerged flow condition. *Flow Measurement and Instrumentation* **81**, 102035. https://doi.org/10.1016/j.flowmeasinst.2021.102035.

Mehrabani Bashar, A., Nozari, H., Marofi, S., Mohamadi, M. & Ahadiiman, A. 2023 Investigation of factors affecting rural drinking water consumption using intelligent hybrid models. *Water Science and Engineering* **16** (2), 175–183. https://doi.org/10.1016/j.wse.2022.12.002.

Nouri, M. & Hemmati, M. 2020 Discharge coefficient in the combined weir–GA te structure. *Flow Measurement and Instrumentation* **75**, 101780. https://doi.org/10.1016/j.flowmeasinst.2020.101780.

Przybył, K. & Koszela, K. 2023 Applications MLP and other methods in artificial intelligence of fruit and vegetable in convective and spray drying. *Applied Sciences* **13** (5), 2965. https://doi.org/10.3390/app13052965.

Rady, R. A. 2016 Modeling of flow characteristics beneath vertical and inclined sluice gates using artificial neural networks. *Ain Shams Engineering Journal* **7** (2), 917–924. https://doi.org/10.1016/j.asej.2016.01.009.

Salas, J. D., Delleur, J. W., Yevjevich, V. & Lane, W. L. 1980 *Applied Modeling of Hydrologic Time Series*. Water Resources Publications, United Kingdom.

Salmasi, F., Nouri, M., Sihag, P. & Abraham, J. 2021 Application of SVM, ANN, GRNN, RF, GP and RT models for predicting discharge coefficients of oblique sluice gates using experimental data. *Water Supply* **21** (1), 232–248. https://doi.org/10.2166/ws.2020.226.

Samantaray, S., Sahoo, A. & Agnihotri, A. 2023 Prediction of flood discharge using hybrid PSO-SVM algorithm in Barak river basin. *MethodsX* **10** (2023), 102060. https://doi.org/10.1016/j.mex.2023.102060.

Sheela, K. G. & Deepa, S. N. 2013 Review on methods to fix number of hidden neurons in neural networks. *Mathematical Problems in Engineering*. https://doi.org/10.1155/2013/425740.

Suntaranont, B., Aramkul, S., Kaewmoracharoen, M. & Champrasert, P. 2020 Water irrigation decision support system for practical weir adjustment using artificial intelligence and machine learning techniques. *Sustainability* **12** (5), 1763. https://doi.org/10.3390/su12051763.

Tao, H., Jamei, M., Ahmadianfar, I., Khedher, K. M., Farooque, A. A. & Yaseen, Z. M. 2022 Discharge coefficient prediction of canal radial gate using neurocomputing models: an investigation of free and submerged flow scenarios. *Engineering Applications of Computational Fluid Mechanics* **16** (1), 1–19. https://doi.org/10.1080/19942060.2021.2002721.

Xing, W. Y., Bai, Y. L., Ding, L., Yu, Q. H. & Song, W. 2022 Application of a hybrid model based on GA–Elman neural networks and VMD double processing in water level prediction. *Journal of Hydroinformatics* **24** (4), 818–837. https://doi.org/10.2166/hydro.2022.016.

Yaghoubzadeh-Bavandpour, A., Rajabi, M., Nozari, H., Ahmad, S., 2022 Support vector machine applications in water and environmental sciences. In: *Computational Intelligence for Water and Environmental Sciences. Studies in Computational Intelligence*, Vo, 1043 (Bozorg-Haddad, O. & Zolghadr-Asli, B., eds). Springer, Singapore, pp. 291–310. https://doi.org/10.1007/978-981-19-2519-1_14.

Yao, Z., Xu, J. P., Kong, J. L. & Liu, S. B. 2018 Prediction of river water level by GA-Elman model. *Journal of Yangtze River Scientific Research Institute* **35** (9), 34–37.

Zaini, N., Malek, M. A., Yusoff, M., Mardi, N. H. & Norhisham, S. 2018 Daily river flow forecasting with hybrid support vector machine–particle swarm optimization. *IOP Conference Series: Earth and Environmental Science, IOP Publishing Ltd.* **140** (2018), 1315–1755. https://doi.org/10.1088/1755-1315/140/1/012035.

Zhang, L. J. & Yuan, D. 2008 Stock market forecasting research based on GA-Elman neural network. *East China Econ Management* **22** (9), 79–82.

Zhou, F., Zou, L., Liu, X., Zhang, Y., Meng, F., Xie, C. & Zhang, S. 2021 Microlandform classification method for grid DEMs based on support vector machine. *Arabian Journal of Geosciences* **14**, 1269. https://doi.org/10.1007/s12517-021-07596-0.

First received 23 November 2022; accepted in revised form 15 June 2023. Available online 24 June 2023